

Randomized, Controlled Histologic and Histomorphometric Evaluation of Implants With Nanometer-Scale Calcium Phosphate Added to the Dual Acid-Etched Surface in the Human Posterior Maxilla

Giovanna Orsini,* Maurizio Piattelli,* Antonio Scarano,* Giovanna Petrone,* James Kenealy,[†] Adriano Piattelli,* and Sergio Caputi*

Background: Placement of dental implants in the posterior maxilla has been associated with higher rates of failure that are due, in part, to the poor bone quality of this region. The purpose of the present study was the histologic and histomorphometric evaluation of the bone around a new implant surface treatment created by a deposition of nanometer-sized calcium phosphate particles added to the dual acid-etched surface.

Methods: One custom-made 2 × 10-mm site evaluation implant (SEI) with this novel treatment surface (test) and one SEI with the dual acid-etched surface without treatment (control) were placed in the posterior maxilla of 15 patients. All SEIs were retrieved after 2 months and evaluated under confocal laser scanning microscopy (CLSM) and by light microscopy for histomorphometric analysis of the bone-implant contact (BIC).

Results: Histologic observations in control SEIs showed formation of new bone around the implant surface; however, it was not always in direct contact with the entire perimeter of the threads. The mean BIC was 19% ± 14.2%. Test SEIs showed peri-implant bone tightly contacting the implant surface and better adapted to the threads. Three-dimensional reconstruction of sections obtained using CLSM showed the intimacy of the contact between bone and test SEI surface through the entire thickness of the specimens. The mean BIC was 32.2% ± 18.5%.

Conclusions: After 2 months of healing, comparison of the BIC values showed a statistically significant greater mean BIC for test SEIs than for controls. The clinical implications of these results included shortening of the implant healing period and earlier loading protocols. *J Periodontol* 2007;78:■■■-■■■.

KEY WORDS

Dental implants; histology; laser; maxilla.

Posterior regions of the maxilla are associated with greater variations in bone quality (density of cancellous bone and thickness of the cortical layer) than anterior regions. Placement of dental implants in the posterior maxilla has been associated with higher rates of integration failure that are due, in part, to the poorer bone quality.¹ Using histomorphometry to measure the percentage of bone-implant contact (BIC) is an established method to determine the extent of osseointegration and the rate of healing of dental implants. Experimental studies in animal models showed that implants with roughened surfaces had a better early anchorage in bone tissue and a higher percentage of BIC than implants with smooth surfaces.²⁻⁶ These results also were demonstrated in human studies.⁷⁻¹² A recent article¹³ documented osseointegration of implants with different rough surfaces after an insertion period <2 months, even when placed in soft bone of the human mandible and maxilla.

The successful clinical use of implants with microrough titanium surfaces has paved the way for developing further

* Operative Unit of Stomatology and Oral Science of Center for Excellence on Aging - "G. d'Annunzio" University Foundation and Department of Stomatology and Oral Science, University of Chieti-Pescara, Chieti, Italy.

[†] Clinical Research, 3i Implant Innovations, Palm Beach Gardens, FL.

surface topographies to promote enhanced peri-implant bone apposition during the early stages of bone regeneration. Buser et al.¹⁴ reported a significantly greater BIC at 2 and 4 weeks of healing in implants with a chemically modified sand-blasted acid-etched (SLA) surface compared to the standard SLA surface. The same group demonstrated that another modification of the SLA surface (polymer coatings) also may improve osseointegration during the initial phases of healing.¹⁵

In addition to the effects of surface topography and surface chemistry, thin deposits of hydroxyapatite (HA) and calcium phosphate (CaP) crystals on implant surfaces accelerated early bone formation and increased the strength of the bond between implant and bone.¹⁶ The HA crystallinity and the application technique were variables that affected the implant–bone interface.¹⁶

To assess the rate and extent of implant healing in humans, custom-made small implants with opposite sides featuring different surface topographies, referred to as site evaluation implants (SEIs), were introduced by Lazzara et al.⁸ and used in subsequent studies.^{11,12} The SEIs were inserted in the posterior maxilla at the time of surgery for placement of clinical implants (prosthesis-supporting implants). They were allowed to heal submerged until second-stage surgery, at which time they were retrieved by trephine for histologic processing. Results of these studies showed that the surface modified by dual acid-etching treatment[‡] increased the extent of adherent new bone compared to a machined surface.

The aim of the present study was a histologic and histomorphometric evaluation of the implant–bone interface to determine the effects of a novel surface treatment, created by discrete crystalline deposition (DCD) of nanometer-sized CaP particles onto the dual acid-etched surface.[§] A confocal laser scanning microscope (CLSM) was used to evaluate serial optical sections of the undecalcified ground sections and to reconstruct the three-dimensional images of the peri-implant bone tissue.^{17,18}

The bone–implant contact percentages for a control group of SEIs featuring only dual acid-etched surfaces (control) were compared to a group of CaP-treated SEIs (test).

MATERIALS AND METHODS

Study Design

This prospective, randomized, controlled, double-blind study evaluated 15 patients (mean age: 56.9 years) enrolled between February 2005 and July 2005 with partial or full edentulism who had elected to receive dental implants to restore their dentition. The protocol was approved by the Ethics Committee of the University of Chieti-Pescara, and all patients provided writ-

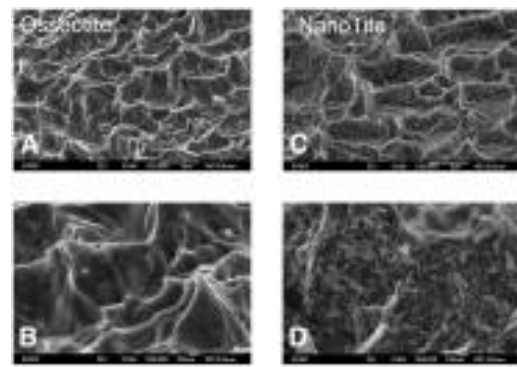


Figure 1.

SEM images of the dual acid-etched surface of the control SEI at low ($\times 20,000$) (A) and high magnification ($\times 50,000$) (B). Surface modification of the test SEI by a discrete deposition of nanometer-sized CaP particles at low ($\times 20,000$) (C) and high magnification ($\times 50,000$) (D).

ten informed consent. Study implants consisted of custom-manufactured 2×10 -mm SEIs with a dual acid-etched surface.^{||} Controls consisted of SEIs with dual acid-etched surfaces without further treatment. Test SEIs had a nanometer-scale CaP DCD surface.[¶] Images of the control and test surfaces (Fig. 1) were made with a scanning electron microscope (SEM).[#] Patients received one of each type of SEI, placed on contralateral sides or on the same side in the posterior maxilla, distal to clinical definitive implants. Control and test SEIs look identical and were differentiated by a batch number on the external package, which was handled only by the surgeon's assistant. A randomization scheme was followed for the placement of test and control implants to ensure balance. The 15 patients were treated with a total of 40 clinical implants** in the maxillary arches, which were to be restored to support final prostheses.

Inclusion criteria were patients of either gender and any race >18 years of age who needed dental implants for treating a fully or partially edentulous maxilla, where the SEI might be placed at positions just distal or near the terminal posterior clinical implants or patients who needed maxillary sinus augmentation procedures prior to clinical implant placement and might have SEI placed in the posterior maxilla at the time of this surgery. Exclusion criteria were active infection or severe inflammation in the area intended for implant placement, uncontrolled diabetes mellitus, metabolic bone disease, or radiation therapy to

‡ Osseotite, 3i Implant Innovations, Palm Beach Gardens, FL.

§ NanoTite, 3i Implant Innovations.

|| Ti-6Al-4V-ELI (Ti-alloy), Osseotite.

¶ NanoTite.

LEO 435 Vp, LEO Electron Microscopy, Cambridge, U.K.

** Osseotite Certain, 3i Implant Innovations.

the head and neck region within the past 12 months, and pregnancy.

Surgical and Clinical Procedures

Patients enrolled in the study were seen initially for clinical evaluation and for collection of demographic, medical, and dental data. Panoramic radiographs and computerized tomographic scans of existing dentition were obtained. SEI placement took place prior to or at the time of clinical implant placement or at the time of the sinus-lifting procedure, through a small-diameter gingival punch or a small flap. A 1.3-mm twist drill was used to prepare the placement site, and SEIs were inserted using a standard driver (Fig. 2A). At least 1 mm of the coronal portion of the implant remained supra-crestal (Fig. 2B). Clinical implants were placed using osteotomy preparation techniques described in the manufacturer's surgical manual (Fig. 3). During drilling, the bone density was recorded based on the surgeon's perception of drilling resistance.^{19,20} Moreover, the quality of initial implant fit was scored as fol-

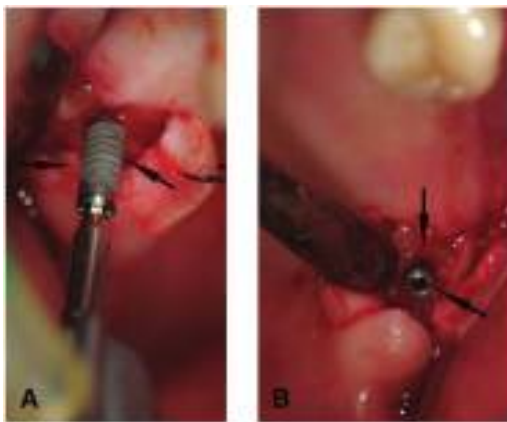


Figure 2.

A) Clinical image of SEI placement (arrows) in the posterior edentulous maxilla of a patient. **B)** At least 1 mm of the coronal portion of the implant (arrows) remains supra-crestal.

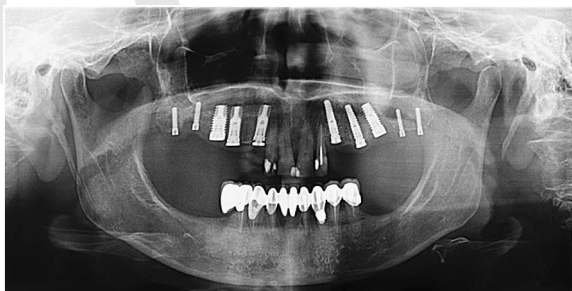


Figure 3.

Panoramic radiograph showing four SEIs placed distally to clinical implants in the posterior region of the maxilla.

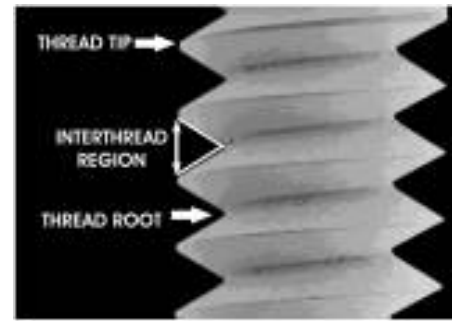


Figure 4.

Drawing of an SEI showing the interthread region; the innermost diameter of the thread, defined as "root"; and the maximum diameter of the thread, defined as "tip."

lows: 1 = tight; 2 = firm; and 3 = loose. After 8 ± 1 weeks of healing, a guide post was attached to the SEI, and the implants were removed using a trephine with an internal diameter of 4 mm. The retrieved specimens were processed for histologic and histomorphometric analysis to determine the percentage of BIC.

Histologic Specimen Processing and Histomorphometrics

The retrieved specimens were fixed immediately in 10% buffered formalin and processed to obtain thin ground sections.²¹ The specimens were dehydrated in graded concentrations of ethanol and embedded in resin.^{††} After polymerization, the specimens were sectioned along the longitudinal axis, with a high-precision diamond disk at about 150 μm , and ground down to $\sim 50 \mu\text{m}$ with a specially designed grinding machine.^{‡‡} The slides were stained with acid fuchsin and toluidine blue. The slides were observed in normal transmitted light;^{§§} qualitative assessments included the proportion of new bone within the interthread region (Fig. 4). Other regions where bone was described included areas referred to as "roots" (the innermost or deepest minimal diameters of the threads) and "tips" (the maximum diameters of the implant threads) (Fig. 4). A CLSM^{|||} was used to take optical images of each ground section, setting the excitation wavelength at 488 nm. The peri-implant soft tissue was detected using a bandpass (BP) 505- to 530-nm filter, and peri-implant bone was detected through a BP 585- to 615-nm filter. Three-dimensional reconstruction was performed from the serial optical sections in a Z interval of 1.4 μm using software.^{¶¶}

†† LR White, London Resin, Berkshire, U.K.

‡‡ Precise 1 Automated System, Assing, Rome, Italy.

§§ Laborlux Microscope, Leitz, Wetzlar, Germany.

||| LSM 510 META, Zeiss, Jena, Germany.

¶¶ Imaris 4.2.0, Bitplane AG, Zurich, Switzerland.

Histomorphometry was performed using the light microscope connected to a high-resolution video camera^{##} and interfaced to a monitor and a computer.^{***} This optical system was associated with a digitizing pad^{†††} and a commercially available histometry software package with image capturing capabilities.^{†††} Computer-based histomorphometric image analyses were performed to determine the linear amount of bone contacting the implant surface on each section. The measurements were used to quantify the percentage of adherent bone contacting the subcrestal portion of the implant where surfaces were exposed to the osseous tissue.

Statistical Analysis

The histomorphometric data for each specimen were recorded as percentage and means for the control and test groups \pm SD. Two sets of tests were applied to the percentage of BIC data originating from each slide. Control and test SEIs were grouped by patient and analyzed using all data and from data eliminating the zero values presumed to have been caused in error during implant recovery. Each data set was analyzed using a paired *t* test. Because the distribution of the differences was skewed slightly, the Wilcoxon signed-rank test also was applied as a measure of robustness.

Because the nanometric CaP surface treatment was exploratory, a two-sided analysis was considered appropriate (probability $>|t|$). However, the assumption could be made that the test-surface treatment would either have a positive or no different effect on BIC as did the control. For this reason, the one-sided *P* value (probability $>t$) also was reported. All analyses were conducted using commercially available software.^{§§§}

RESULTS

Control and Test SEI Surgeries

Fifteen patients (11 men and four women) with a mean age of 56.9 years met the inclusion criteria. Of the 15 patients who received SEIs, nine patients received one of each type (control and test) of SEI at the time of implant placement surgery for clinical implants. Five other patients received one of each type of SEI in the posterior region of the maxilla at the time of maxillary sinus augmentation procedures, and one patient received four SEIs (two tests and two controls) during bilateral sinus-lifting surgery (Fig. 2); therefore, 32 SEIs (16 test SEIs and 16 control SEIs) were placed. All SEIs were placed in the posterior region of the maxilla, distal to the sites chosen for placement of definitive clinical implants; none were placed in sinus-augmented sites. All patients were treated with clinical implants: 22 implants were placed in the maxillae of nine subjects who did not require augmentation procedures, and 18 implants were placed in six sub-

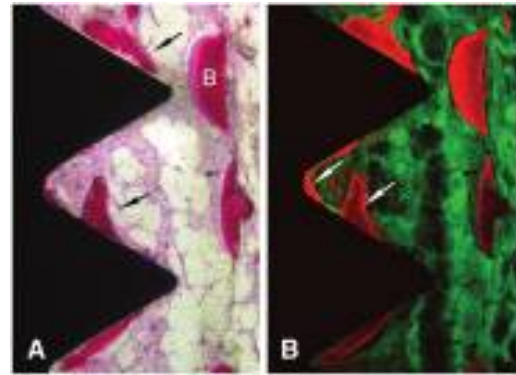


Figure 5.

A) Histologic view of control SEI. Osteoconductivity is present; however, bone (B) sometimes grew far from the implant surface. There are a few bone trabeculae (arrows) in the interthread region. (Acid fuchsin and toluidine blue; original magnification $\times 10$.) **B)** The CLSM image reveals an initial thin bone layer in contact with the thread root (arrows) (original magnification $\times 10$).

jects who underwent sinus augmentation procedures using a porcine-derived bone substitute^{||||} 5 months before implant placement.

At the time of SEI surgeries, the bone density scores indicated low-density bone (type D3-D4) in all cases. The implant fit was registered as 2 (firm) for 29 of the 32 implants; in three cases, the implant fit was recorded as 3 (loose). Healing in all surgical sites progressed normally and without complication or exposure of control or test SEIs. After a mean healing time of 8 ± 1 weeks, SEIs and surrounding hard and soft tissue were retrieved by trephine drill. At the time of removal, possible cutting artifacts were suspected in two samples. One control SEI and one test SEI were harvested without the surrounding bone.

Histologic and Histomorphometric Results

Evaluation of control SEIs. Histology from the harvested control SEIs showed predominantly D3-D4 bone quality with a small amount of mineralized bone matrix in areas around the implant. Osteoconductivity was observed; however, new bone was growing about 0.1 to 0.3 mm from the implant surface in some cases (Fig. 5A). In these cases, there was a lack of direct connecting bridges between the peri-implant bony trabeculae and the implant surface.

CLSM showed only a few regions in which bone was in close contact with the implant roots (Fig. 5B); in other regions, bone appeared to end in a somewhat

3CCD, JVC KY-F55B, JVC, Yokohama, Japan.

*** Intel Pentium III 1200 MMX, Intel, Santa Clara, CA.

††† Matrix Vision GmbH, Oppenweiler, Germany.

†††† Image-Pro Plus 4.5, Media Cybernetics, Immagini & Computer, Milan, Italy.

§§§ JMP v5.0.1, SAS Concepts, Cary, NC; and SAS v8.2, SAS Institute, Cary, NC.

|||| Apatos Tecness, Turin, Italy.

perpendicular orientation to the implant surface (Fig. 6A), and it was starting to grow in the interthread region, without coming into direct contact with the implant roots (Fig. 6B). In general, control SEIs were characterized by trabecular bone with wide marrow spaces and large osteocytic lacunae, and peri-implant bone was not always continuous and rarely followed the entire perimeter of the threads (Fig. 6). Large-diameter blood vessels and small capillaries were present between the bone trabeculae (Fig. 6A). Resorption lacunae were absent at the apex of the threads, and no bone remodeling was observed.

Three-dimensional reconstruction of the serial optical sections obtained by CLSM showed a slight difference in the bone presence throughout the thickness of the histologic slide. For example, when examining the section from above, there was no bone formation in the implant root (Fig. 7A), whereas, when viewing the section from below, initial osteogenesis was evident (Fig. 7B).

At the apexes of nine implants, mainly marrow spaces and a few bone trabeculae were present; most bone trabeculae were not in direct contact with the implant surface. In six implants there was a lack of bone in the apical third of the implant surface. No acute inflammatory cell infiltrates were present. No gaps or dense fibrous connective tissue were present, except in four cases in which a thin layer of connective tissue was observed in contact with some threads of the coronal and middle portion of the implant surface. In three cases, there was an apical epithelial downgrowth to the first two implant threads. There was one control SEI in

which no bone material was present in the entire section, suggesting a trephine removal artifact.

The BIC values and summary data for the control specimens, including and excluding the patients with suspected artifacts, are presented in Table 1. Excluding patients with suspected artifacts, the mean BIC percentage for the control SEI group was 19.0% ± 14.18%.

Evaluation of test SEIs. Histology of the harvested test SEIs with the surrounding tissue showed that

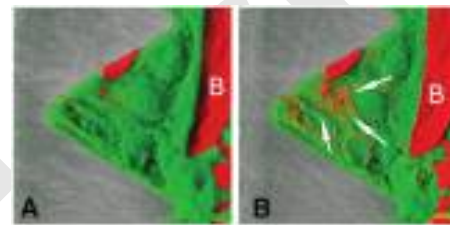


Figure 7. Three-dimensional reconstruction of the interthread region of a control SEI obtained from serial optical sections using CLSM allowed evaluation of the entire thickness of the undecalcified specimen. **A)** When examining the histologic slide from above, there is bone (B) ~0.1 mm from an implant tip and almost no evidence of bone in the thread root. **B)** When viewing the slide from below, some bone formation (arrows) can be detected. (Original magnification: A and B, ×20.)

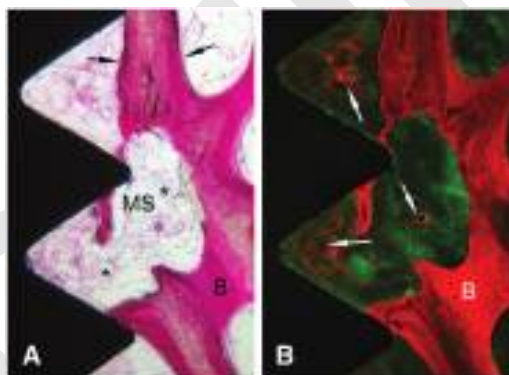


Figure 6. **A)** Histologic view of control SEI. It is possible to observe trabecular newly formed bone with wide marrow spaces (MS) containing numerous blood vessels (*). The bone surrounding the implant appears to end in a somewhat parallel orientation (arrows) to the implant surface, and there is a lack of direct connecting bridges between the peri-implant bone trabeculae and the implant surface. (Acid fuchsin and toluidine blue; original magnification ×10.) **B)** The CLSM image reveals initial bone deposition in the interthread region (arrows); however, no bone-implant contact was present at the level of the thread root (original magnification ×10).

Table 1. Summary of BIC for Control SEIs

Patient Number	BIC (%)	
1	4.3	
2	54.1	
3	40.0	
4	24.0	
5	3.0	
6	15.3	
7	30.3	
8	19.6	
9	8.1	
10	7.2	
11 (case 1)	9.8	
11 (case 2)	19.8	
12	53.1	
13	13.0	
14	18.1	
15	0	
Summary	Excluding Patients With "0" Values	
N	16	14
Mean	20.0	19.0
SD	16.71	14.18
Minimum	0	3.0
Maximum	54.1	53.1

preexisting bone in the posterior region of the maxilla was type D3-D4 with large marrow spaces. The first BIC was located ~2 mm from the shoulder of the implant; epithelial and connective tissue cells were found in this area. The newly formed bone, which had a higher affinity for dyes, was in tight contact with the implant surface and adapted perfectly to the microirregularities of the implant surface (Fig. 8A). This bone did not end perpendicular to the implant surface, but gradually became thinner as it extended toward the crest of the threads (Fig. 8A). Confocal microscopy allowed a better focused image showing the numerous osteocytic lacunae present in the peri-implant bone and the new bone formation in the interthread region (Fig. 8B).

The bone contacting the implant surfaces was composed primarily of woven bone that was connected to the preexisting bone by newly formed bony trabeculae (Fig. 9A). The layers of newly formed bone appeared to have formed from the implant surface toward the original bone bed. There were regions of newly formed bone, and areas of bone maturation, expressed by lamellar compaction, also were present (Fig. 9). Sometimes, details of the peri-implant bone formation were more evident in CLSM images (Fig. 9B). For implant surface areas that were located in marrow spaces, a continuous layer of bone circumscribed the marrow spaces well. Some solitary bone bridges originated from the implant surface with an outward direction toward the marrow spaces (Fig. 10A). There were marrow spaces that surrounded the tips of the implant threads (Fig. 10A), whereas other implant tips were in direct contact with bone (Fig. 10B). Sometimes, osteoblasts were found near the bone trabeculae located on the implant surface.

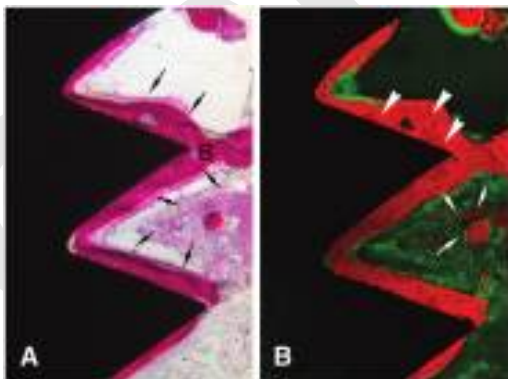


Figure 8.

A) Histologic view of test SEI. The bone (B) is adapted well to the entire perimeter of the implant threads (arrows). (Acid fuchsin and toluidine blue; original magnification $\times 10$.) **B)** The CLSM image allows improved identification of osteocytes (arrowheads) in the peri-implant bone and helps in the detection of some newly formed bone in the interthread region (arrows) (original magnification $\times 10$).

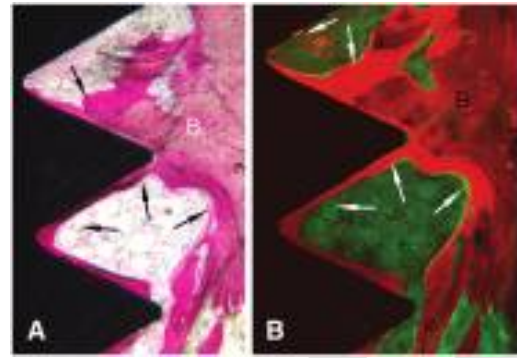


Figure 9.

A) Histologic view of test SEI. Preexisting bone (B) is connected to the newly formed bony trabeculae that are in close contact with the implant surface (arrows). (Acid fuchsin and toluidine blue; original magnification $\times 10$.) **B)** The CLSM image reveals details of the newly formed bone closely adherent to the implant surface (arrows) (original magnification $\times 10$).

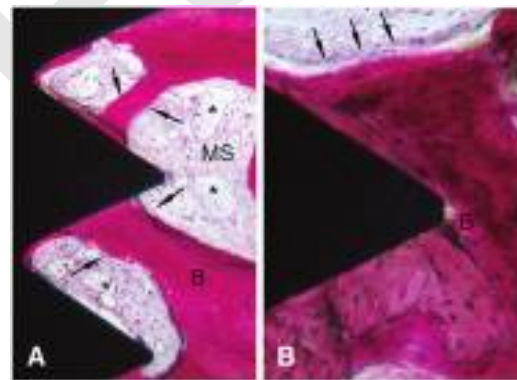


Figure 10.

A) Histologic view of test SEI. There is a continuous layer of bone (B) on the implant surface, and numerous marrow spaces (MS), presenting large blood vessels (*), are circumscribed well by the newly formed bone. Bone bridges (arrows) originating from the implant surface have an outward direction toward the original bone bed. **B)** Compact bone (B) is in close contact with an implant tip. At this magnification, it is possible to observe a rim of osteoblasts (arrows) depositing osteoid matrix that is undergoing mineralization. (Acid fuchsin and toluidine blue; original magnification, A $\times 10$; B, $\times 20$.)

These osteoblasts actively were depositing osteoid matrix that also was undergoing mineralization (Fig. 10B). Many large-diameter blood vessels and numerous small capillaries were present between the bone trabeculae (Fig. 10A).

Three-dimensional reconstruction of the serial optical sections obtained under CLSM showed the different degrees of bone formation in the interthread region through the thickness of the histologic section. For example, when examining the slide from above there was slightly less bone formation (Fig. 11A) than when viewing the slide from below (Fig. 11B).

At the apexes of 10 implants, marrow spaces and a few bone trabeculae in close contact with the implant surface were present. In five implants, there was a lack of bone in the apical third of the implant surface. No infrabony pockets, active bone resorption, or osteoclasts were present. No acute inflammatory cell infiltrates were observed. There were no gaps or dense fibrous connective tissue at the bone–implant interface. Only in two cases was there apical epithelial downgrowth to the first two implant threads. There was one test SEI in which no bone material was present in the entire section, suggesting a trephine removal artifact.

The BIC values and summary data for all test specimens, including and excluding the patients with suspected artifacts, are presented in Table 2. Excluding patients with suspected artifacts, the mean BIC percentage for the test SEI group was 32.2% ± 18.49%.

Statistical Results

The following statistical results summarized the comparisons (Table 3). When examining all of the data, the test SEIs showed a greater BIC percentage (mean Δ = 9.24%). However, the paired *t* test indicated that the difference was not statistically significant at the 0.05 level (*P* = 0.2021). When zero contact values were eliminated, the test SEIs also showed a greater BIC percentage (Δ = 13.26%), and the two-sided paired *t* test indicated a trend toward statistical significance (*P* = 0.0554). The Wilcoxon signed-rank tests supported these findings (*P* = 0.1439 for the full dataset; *P* = 0.0580 for the dataset excluding “0” values). If the assumptions for a one-sided test were made, the results were significant at the 0.05 level (paired *t* test, *P* = 0.0277; Wilcoxon signed-rank test, *P* = 0.0290) for the dataset excluding patients with suspected artifacts.

DISCUSSION

To our knowledge, this study is the first human, histologic evaluation of the early healing process of an

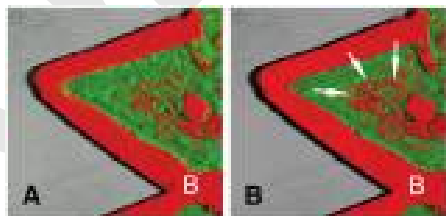


Figure 11.

Three-dimensional reconstruction of the interthread region of a control SEI obtained from serial optical sections using CLSM. Often, bone (B) is found extending into the internal profile of the interthread region. If the reconstruction of the histologic section is seen from above (A), there is slightly less bone formation (arrows) than if the slide is viewed from below (B). (Original magnification ×20.)

Table 2.

Summary of BIC for Test SEIs

Patient Number	BIC (%)	
1	45.1	
2	0	
3	52.0	
4	65.1	
5	23.0	
6	22.4	
7	15.0	
8	47.7	
9	53.1	
10	47.0	
11 (case 1)	19.0	
11 (case 2)	13.5	
12	22.0	
13	7.1	
14	19.0	
15	16.3	
Summary	Excluding Patients With “0” Values	
N	16	14
Mean	29.2	32.2
SD	19.31	18.49
Minimum	0	7.1
Maximum	65.1	65.1

Table 3.

Statistical Analysis of Treatment Difference in BIC Percentage

Summary	Including “0” Values	Excluding “0” Values
N	16	14
Mean difference	9.24	13.26
SD of difference	27.69	23.57
Minimum difference	−54.06	−31.05
Maximum difference	44.98	44.98
<i>P</i> value (two-sided paired <i>t</i> test)	0.2021	0.0554
<i>P</i> value (one-sided paired <i>t</i> test)	0.1010	0.0277
<i>P</i> value (two-sided Wilcoxon signed-rank)	0.1439	0.0580
<i>P</i> value (one-sided Wilcoxon signed-rank)	0.0720	0.0290

implant surface treated with DCD of nanometer-scale CaP particles on the dual acid-etched microtopographic surface. The study was designed to determine BIC and the pattern of bone growth after 2 months of unloaded

healing in the posterior maxilla for SEIs with a CaP-treated surface compared to SEIs with an unmodified dual acid-etched surface.

To ensure balance and to minimize differences in bone density and patient biology, test and control implants were placed in the same patient, using a randomization scheme, in close proximity to each other in the same side of the posterior maxilla or in contralateral sites in the most distal region possible of the posterior maxilla. The bone scores recorded during osteotomy drilling showed that all of the SEI recipient sites had low-density bone (D3-D4). Upon histologic examination, the bone showed few bone trabeculae over the total bone area, including the marrow spaces.

Longitudinal, descriptive human studies, as well as histologic data, indicate that the clinical success rates for endosseous implants vary according to anatomic location.⁷ In general, areas with higher quality bone have greater success rates compared to areas with reduced bone quality, such as the posterior maxilla. Modification of an implant surface, by producing a topographically rougher texture, was shown to result in greater BIC. For the dual acid-etched surface, a higher BIC rate in areas of poor bone quality was reported compared to a machined surface.^{5,8,11,12,22,23} A meta-analysis of clinical studies of dual acid-etched implants placed in poor quality bone indicated that these implants can be used in soft bone without compromising implant performance or duration of failure-free function.²⁴

Roughening the topography of the implant by applying thin crystalline deposits of HA or CaP increased implant performance and survival rates.^{25,26} Although concerns have included the potential dissolution and detachment of HA coatings,^{27,28} Trisi et al.²⁹ showed that for two HA-coated implants that were retrieved after 10 years of functional loading, most of the surface coating maintained its structural integrity. Any disappearance of HA from the implant surface was minimal and was not associated with the absence of BIC; therefore, osseointegration did not seem to be compromised. CaP may exhibit different dissolution and reprecipitation properties that may enhance early bone formation and bone bonding,^{30,31} and crystallinity or phosphate groups may play a role in apatite formation.^{32,33} A recent report demonstrated that very thin CaP deposits of different crystallinities, produced by a low-temperature deposition process, resulted in high BIC percentages and high interfacial strengths in rats after 3 and 9 weeks of healing.¹⁶ In the present study, the process used to produce the test surface added CaP crystals ranging in length from 20 to ~100 nm. Because the crystals are affixed to the surface as discrete deposits, there is no confluent layer or coating that is subject to delamination or detachment.

The comparison of BIC values for the CaP-treated surface and the dual acid-etched surface showed a mean BIC for the test group (32.2%) that was greater than the mean BIC for the control group (19.0%). Statistical analysis showed that this difference indicated a trend in favor of the test surface. Under the assumptions of a one-sided paired *t* test, the difference was significant. When patients who had suspected artifacts were included, the test group mean (29.2%) was greater than that for the control group (20.0%); however, this difference was not statistically significant.

The histomorphometric evaluations of the specimens revealed that the highest BIC value recorded, 65%, was for a test implant; the highest BIC recorded for any control implant was 54%. With the exception of one test BIC value that was zero due to an error during harvesting, only one test SEI had a BIC value <10%, whereas four control SEIs had BIC values <10%. In 10 of 14 (71%) SEIs where a non-zero BIC value was detected, the test SEIs had a higher BIC percentage than the control SEIs.

These data are comparable with data from human histologic studies by Lazzara et al.⁸ and Trisi et al.,^{11,12} in which custom-made SEIs with split surfaces (one side featured a dual acid-etched surface and the opposite side had a machined surface) were placed in the posterior maxilla. After 2 months of healing, Trisi et al.¹² reported a mean BIC of 47.8% for the dual acid-etched surface, whereas the mean BIC in the present study was 18.9%. However, the length of the SEI used in those studies was half (5 mm) that of the SEI in the present study; this fact may account for the lower BIC values. In the case of a 5-mm implant, approximately half of the implant is in contact with the crestal cortical bone, and the apical half is surrounded by cancellous bone. Often, the posterior maxilla is dominated by a loose structure of the cancellous substance with a thin crestal cortical bone with openings into marrow spaces.³⁴ Generally, the cancellous bone structure is poor, and because the molars are lost at a relatively early stage, the atrophy-related resorptive process commences earlier and progresses further in this region.³⁴ For a 10-mm implant, only ~20% of the implant surface is in contact with the cortical bone; the remaining 80% is located within trabecular bone where lower BIC percentages would be anticipated. In similarly designed studies, Lazzara et al.⁸ and Trisi et al.¹¹ also reported a greater mean BIC value for the dual acid-etched surface compared to the machined surface when using 5-mm-long SEIs that were allowed to heal for 6 months.

A very interesting finding was the different pattern of bone growth observed by CLSM around test and control implants. Conventional light microscopy always reaches its limits when the emission signals of

the dyes overlap. Confocal microscopy scans the specimen pixel by pixel and line by line, assembling an image that is an optically thin section through the specimen.¹⁷ Because the titanium implant was hard to cut, and because the border between bone tissue and implant could be broken easily during preparation, thick undecalcified sections were preferable for observing the bone-implant interface.¹⁷ CLSM was helpful in its ability to make optical sections of the specimen, thus distinguishing, by high contrast and better focus, that bone around test SEIs was adapted closely to the implant threads following the principles of contact osteogenesis.³⁵ In addition, the three-dimensional view reconstructed from the images obtained by taking serial optical sections by changing the plane of focus, displayed the stereographic structure of the bone-implant interface through the entire thickness of the histologic slide. For control SEIs, the bone surface facing the implant did not always match the implant profile; sometimes it was observed touching the tips of the implant threads without penetrating into the thread roots, which showed initial osteogenesis only in the central areas of the thread roots. Even in specimens with a low BIC value, the test surface showed the histologic appearance of a continuous layer of bone, "flowing" along the implant surface, which is typical of an osteoconductive surface.⁸

CONCLUSIONS

Within the limitations of the patient sample in this study, BIC evaluations indicated that an increase in osteoconduction along the CaP-treated surface occurs during the first 2 months after implant placement. These results suggested that the nanometric deposition of CaP crystals can be clinically advantageous for shortening the implant healing period, providing earlier fixation, and minimizing micromotion, thus allowing earlier loading protocols and restoration of function for implants placed in areas with low-density bone.

ACKNOWLEDGMENTS

Dr. Kenealy is director of clinical research at 3i Implant Innovations, Palm Beach Gardens, Florida. The authors gratefully acknowledge the assistance of Dr. Simone Guarnieri, researcher, Faculty of Medicine, University of Chieti-Pescara, with CLSM observations. Experimental implants were provided by 3i Implant Innovations, Palm Beach Gardens, FL.

REFERENCES

- Jaffin RA, Berman CL. The excessive loss of Brånemark fixtures in type IV bone: A 5-year analysis. *J Periodontol* 1991;62:2-4.
- Buser D, Schenk RK, Steinemann S, Fiorellini JP, Fox CH, Stich H. Influence of surface characteristics on bone integration of titanium implants. A histomorphometric study in miniature pigs. *J Biomed Mater Res* 1991;25:889-902.
- Gotfredsen K, Nimb L, Hjorting-Hansen E, Jensen JS, Holmen A. Histomorphometric and removal torque analysis for TiO₂-blasted titanium implants. An experimental study on dogs. *Clin Oral Implants Res* 1992; 3:77-84.
- Wennerberg A, Albrektsson T, Andersson B, Krol JJ. A histomorphometric and removal torque study of screw-shaped titanium implants with three different surface topographies. *Clin Oral Implants Res* 1995;6: 24-30.
- Cordioli G, Majzoub Z, Piattelli A, Scarano A. Removal torque and histomorphometric investigation of 4 different titanium surfaces: An experimental study in the rabbit tibia. *Int J Oral Maxillofac Implants* 2000;15: 668-674.
- Piattelli M, Scarano A, Paolantonio M, Iezzi G, Petrone G, Piattelli A. Bone response to machined and resorbable blast material titanium implants: An experimental study in rabbits. *J Oral Implantol* 2002;28:2-8.
- Cochran DL. A comparison of endosseous dental implant surfaces. *J Periodontol* 1999;70:1523-1539.
- Lazzara RJ, Testori T, Trisi P, Porter SS, Weinstein RL. A human histologic analysis of osseointegration and machined surfaces using implants with 2 opposing surfaces. *Int J Periodontics Restorative Dent* 1999;19: 117-129.
- Khang W, Feldman S, Hawley CE, Gunsolley J. A multi-center study comparing dual acid-etched and machined-surfaced implants in various bone qualities. *J Periodontol* 2001;72:1384-1390.
- Davarpanah M, Martinez H, Etienne D, et al. A prospective multicenter evaluation of 1,583 3i implants: 1- to 5-year data. *Int J Oral Maxillofac Implants* 2002; 17:820-828.
- Trisi P, Lazzara R, Rao W, Rebaudi A. Bone-implant contact and bone quality: Evaluation of expected and actual bone contact on machined and osseointegration implant surfaces. *Int J Periodontics Restorative Dent* 2002;22:535-545.
- Trisi P, Lazzara R, Rebaudi A, Rao W, Testori T, Porter SS. Bone-implant contact on machined and dual acid-etched surfaces after 2 months of healing in the human maxilla. *J Periodontol* 2003;74:945-956.
- Iezzi G, Degidi M, Scarano A, Perrotti V, Piattelli A. Bone response to submerged, unloaded implants inserted in poor bone sites: A histological and histomorphometrical study of 8 titanium implants retrieved from man. *J Oral Implantol* 2005;31:225-233.
- Buser D, Brogini N, Wieland M, et al. Enhanced bone apposition to a chemically modified SLA titanium surface. *J Dent Res* 2004;83:529-533.
- Germanier Y, Tosatti S, Brogini N, Textor M, Buser D. Enhanced bone apposition around biofunctionalized sandblasted and acid-etched titanium implant surfaces. *Clin Oral Implants Res* 2006;17:251-257.
- Oh S, Tobin E, Yang Y, Carnes DL Jr., Ong JL. In vivo evaluation of hydroxyapatite coatings of different crystallinities. *Int J Oral Maxillofac Implants* 2005;20: 726-731.
- Suzuki K, Aoki K, Ohya K. Effects of surface roughness of titanium implants on bone remodeling activity of femur in rabbits. *Bone* 1997;21:507-514.
- Lan J, Wang Z, Wang Y, Wang J, Cheng X. The effect of combination of recombinant human bone morphogenetic protein-2 and basic fibroblast growth factor on

- insulin-like growth factor-I on dental implant osseointegration by confocal laser scanning microscopy. *J Periodontol* 2006;77:357-363.
19. Misch C. Classifications and treatment options of the completely edentulous arch in implant dentistry. *Dent Today* 1990;9:26, 28-30.
 20. Trisi P, Rao W. Bone classification: Clinical-histomorphometric comparison. *Clin Oral Implants Res* 1999;10:1-7.
 21. Piattelli A, Scarano A, Quaranta M. High-precision, cost-effective system for producing thin sections of oral tissues containing dental implants. *Biomaterials* 1997;18:577-579.
 22. Klokkevold PR, Johnson P, Dadgostari S, Caputo A, Davies JE, Nishimura RD. Early endosseous integration enhanced by dual acid etching of titanium: A torque removal study in the rabbit. *Clin Oral Implants Res* 2001;12:350-357.
 23. Weng D, Hoffmeyer M, Hurzeler MB, Richter EJ. Osseotite vs machined surface in poor bone quality. A study in dogs. *Clin Oral Implants Res* 2003;14:703-708.
 24. Stach RM, Kohles SS. A meta-analysis examining the clinical survivability of machined-surfaced and Osseotite implants in poor-quality bone. *Implant Dent* 2003;12:87-96.
 25. Block MS, Gardiner D, Kent JN, Misiek DJ, Finger IM, Guerra L. Hydroxyapatite-coated cylindrical implants in the posterior mandible: 10-year observations. *Int J Oral Maxillofac Implants* 1996;11:626-633.
 26. McGlumphy EA, Peterson LJ, Larsen PE, Jeffcoat MK. Prospective study of 429 hydroxyapatite-coated cylindrical omniloc implants placed in 121 patients. *Int J Oral Maxillofac Implants* 2003;18:82-92.
 27. Rohrer MD, Sobczak RR, Prasad HS, Morris HF. Postmortem histologic evaluation of mandibular titanium and maxillary hydroxyapatite-coated implants from 1 patient. *Int J Oral Maxillofac Implants* 1999;14:579-586.
 28. Watson CJ, Tinsley D, Ogden AR, Russell JL, Mulay S, Davison EM. A 3 to 4 year study of single tooth hydroxylapatite coated endosseous dental implants. *Br Dent J* 1999;187:90-94.
 29. Trisi P, Keith DJ, Rocco S. Human histologic and histomorphometric analyses of hydroxyapatite-coated implants after 10 years of function: A case report. *Int J Oral Maxillofac Implants* 2005;20:124-130.
 30. Ong JL, Hoppe CA, Cardenas HL, et al. Osteoblast precursor cell activity on HA surfaces of different treatments. *J Biomed Mater Res* 1998;39:176-183.
 31. Dekker RJ, de Bruijn JD, Stigter M, Barrere F, Layrolle P, van Blitterswijk CA. Bone tissue engineering on amorphous carbonated apatite and crystalline octacalcium phosphate-coated titanium discs. *Biomaterials* 2005;26:5231-5239.
 32. Uchida M, Kim HM, Kokubo T, Fujibayashi S, Nakamura T. Structural dependence of apatite formation on titania gels in a simulated body fluid. *J Biomed Mater Res A* 2003;64:164-170.
 33. Xiropaidis AV, Qahash M, Lim WH, et al. Bone-implant contact at calcium phosphate-coated and porous titanium oxide (TiUnite)-modified oral implants. *Clin Oral Implants Res* 2005;16:532-539.
 34. Ullm C, Kneissel M, Schedle A, et al. Characteristic features of trabecular bone in edentulous maxillae. *Clin Oral Implants Res* 1999;10:459-467.
 35. Davies JE. Understanding peri-implant endosseous healing. *J Dent Educ* 2003;67:932-949.
- Correspondence: Dr. Adriano Piattelli, University of Chieti-Pescara, Via dei Vestini 31, 66013 Chieti, Italy. Fax: 39-0871-3554076; e-mail: apiattelli@unich.it.

Accepted for publication October 6, 2006.